N-Way Spatial Power Combiner Using Tapered Antipodal Slotline Feed Array in a Radial Waveguide

Ilker Karaman[1], Volkan Acikel[2], Murat Koc[3]
Aselsan, Türkiye
[1]ikaraman@aselsan.com.tr, [2]vacikel@aselsan.com.tr, [3]mrtkoc@aselsan.com.tr

***Abstract*— This paper presents a broadband power combining technique based on a tapered microstrip antipodal slot-line feed array in a radial waveguide. The technique also adopts the structure of a broadband conical transmission line to transform the radial waveguide into a 50 Ω coaxial output. The microstrip antipodal slot-line is tapered with an exponential function in order to match the wave impedance of each array element to the radial waveguide impedance. On the output side, a low-loss transition from the radial waveguide to a coaxial transmission line is designed. In this manuscript, a 16-way combiner in the 2–8 GHz operation band is designed and fabricated. The design approach is validated with the simulation and measurement results.**

***Keywords*—radial power combiner, antipodal slotline array, high power rf combiners, rf passive components, rf power amplifiers.**

I. Introduction

In the area of RF and microwave systems, there are many applications that require high output power over a broadband operating frequency bandwidth. For a long time, vacuum tube devices, such as traveling tube amplifiers, klystrons, and magnetrons were the preferred choices for such applications. However, with the recent advancements of solid-state high-power amplifiers (SSPAs) they became an alternative to vacuum devices in exchange for the requirement of multi-device combining [1]. Recently, designing a highly effective and scalable method to combine many amplifiers at wideband operation frequencies has attracted a lot of interest. There are two combining approaches: binary tree-combiners, which combine each two amplifiers in one step, and parallel combiners, which combine all N amplifiers in one step. In the tree-structured power combination, each connecting transmission line segment adds losses and significantly decreases the overall combining efficiency for combiners, especially for higher N [2]. On the other hand, the parallel combiners have a minimized pathway, which results in low loss and high combining efficiency for combining large quantities of amplifiers.

In the last few years, the rectangular waveguide-based spatial power combiner has been developed. However, the cut-off characteristics of rectangular waveguides restrict the operating frequency of this structure. Additionally, non-uniform distribution of TE10 mode inside the rectangular waveguide causes non-uniform distribution both in amplitude and phase in combined ways [3]. The oversized coaxial waveguide for spatial power combining was introduced by Dr. Alexanian and Dr. York to address the above-mentioned drawbacks of the rectangular waveguide combining method [4].

N power amplifiers should be positioned between the inner and outer conductors of the coaxial waveguide with the same angular spacing in order to feed the coaxial waveguide in the power combiner uniformly. This structure comes with the cost of a complex cooling system to overcome the heating problem of SSPAs.

In this paper, the oversized radial waveguide for spatial power combining is presented. The combining technique adopts the structure of a broadband multi-way radial waveguide, which is fed by a 16-tapered microstrip slot-line array. Each input microstrip slot-line provides a gradual transition from the coaxial TEM field to the TEM field of a radial waveguide. At the output side, the signal transmitted through the radial waveguide is transferred to an oversized coaxial waveguide impedance transformation circuitry to feed the coaxial sum port with low loss and low reflection. By using this structure, we aimed to locate 16 power amplifiers on a large planar circular cooling platform that simplifies the cooling system design for power amplifiers.

II. Combiner Design

In an N-way combiner, the impedance of a radial waveguide fed by N parallel antipodal slot-line slices is calculated as 1/N times the impedance of each antipodal slot-line slice, Z_s [2]. In order to couple the energy from 50 Ω inputs to the radial waveguide, in each slice, the 50 Ω input impedance should be matched to Z_s by the use of a tapered antipodal slot-line impedance transformer. For high Z_s/N values, the input impedance transformer circuit becomes challenging to design. For low Z_s/N values, the distance between the inner and outer conductors of the conical transmission line gets shorter, which may lead to a dielectric breakdown problem at high RF power levels. Therefore, Z_s/N is chosen as 37.5 Ω. So, for a 16-way power combiner, Z_s can be found as 600 Ω.

A. The Design of Antipodal Slot-line Impedance Transformer

The antipodal slot-line is a planar two-conductor transmission line, in which the distance between two conductors determines the characteristic impedance. Tapered impedance matching is used to achieve broadband matching from 50 input ports to Zs, so the characteristic impedance of the slot-line is gradually increased from the input port to the end of the slice. The slot-line transformer layout used in this combiner is presented in Fig. 1.

For each N way, the same tapered slot-line transformer is used. Hence, a symmetric and uniform loading around the radial transmission line is achieved. Due to the symmetric

loading and dominant mode excitation, the solution domain can be reduced to a rectangular cross-sectional cell with perfect electrical conductor (PEC) and perfect magnetic conductor (PMC) boundary conditions applied in Fig. 2. Each unit cell is left with one tapered slot-line and a parallel-plate waveguide structure [5], [6].

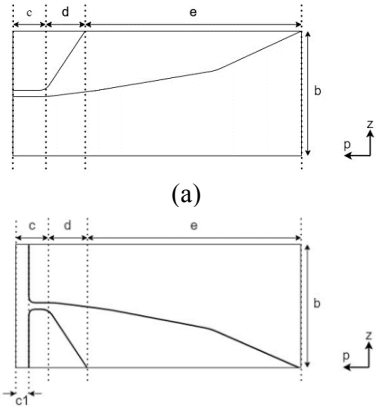

Fig. 1. (a) The top layer of tapered slot-line impedance transformer design, (b) the bottom layer of tapered slot-line impedance transformer design.

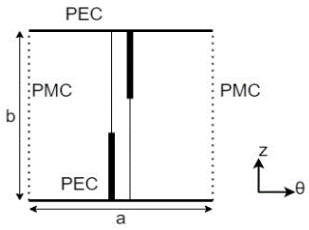

Fig. 2. The boundary conditions applied on the unit cell of tapered slot-line impedance matching structure.

For the unit cell shown in Fig. 1 and Fig. 2, the impedance is calculated and optimized over the frequency band of 2 GHz to 8 GHz in the High Frequency Structure Simulator (HFSS) simulation. The results are presented in Fig. 3.

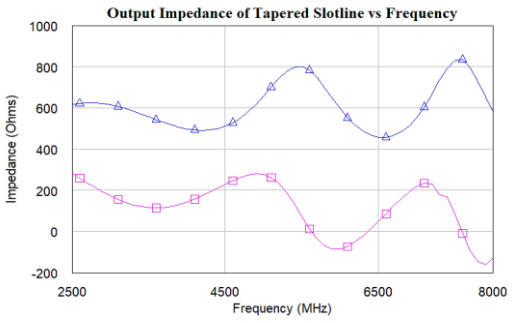

Fig. 3. Obtained output impedance of tapered slotline transformer vs. frequency graphs.

As shown in Fig 3. the tapered antipodal slotline impedance transformer has a ratio of 1:12 and it transforms 50 Ω input impedance to approximately 600 Ω at a broadband operating frequency band. The design parameters of the designed tapered slotline transformer are presented in Table 1.

Table 1. The obtained dimensional values of the designed slotline taper which are shown in Fig. 1.

Parameter	Length (mm)
a	30
b	18.9
c	6.2
c1	3.1
d	5
e	43.8

B. The Design of Conical Transmission Line to Oversize Coaxial Waveguide Transition

The next step in our design is to achieve a smooth transition between the conical transmission line and the oversize coaxial waveguide stage. The impedance transition structure for a conical waveguide to a coaxial waveguide is shown in Fig 4 [7].

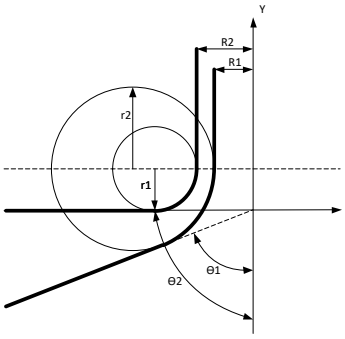

Fig. 4. Conical to coaxial transmission line constant impedance transition structure.

If the characteristic impedance of free space is approximated to 120 π, the characteristic impedance of a conical transmission line operating in TEM mode could be found as in (1) [7], [8].

$$Z_0 = 60\ln\frac{\tan(\theta_2/2)}{\tan(\theta_1/2)} \quad (1)$$

For a smooth transition, the impedance of Z_s/N, and the characteristic impedance of a conical transmission line should be equal in order to minimize the reflection between these two transmission mediums.

To secure the symmetric signal distribution of N inputs around the center of the combiner, θ_2 for our design should be 90°. The impedance of conical transmission line Z_s /N for our design is calculated as 37.5 Ω. Then, the value of θ_1 is found to be 56.3° and it is applied to our design geometry as shown in Fig. 5.

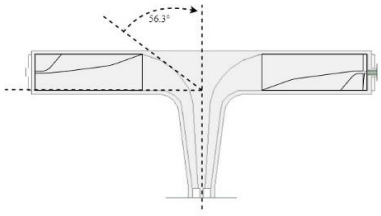

Fig. 5. The designed transition between radial waveguide to conical transmission line.

The characteristic impedance of an air dielectric coaxial line is given as in (2) [7].

$$Z_0 = 60\ln\frac{R_2}{R_1} \quad (2)$$

R2 and R1 values are chosen as 10.5mm and 5.6mm, respectively, to have 37.5 Ω characteristic impedance at the input side of the conical coaxial transmission so low-reflection profile in the structure could be obtained.

We are choosing R_2 to be 10.5mm, and the R_1 value is calculated to be 5.6mm to reach 37.5 Ω characteristic impedance at the input side of the coaxial waveguide and create a low-reflection profile in the structure.

C. The Design of Coaxial Waveguide Impedance Transformer

The tapered coaxial waveguide is designed at the output side to match the 37.5 Ω impedance to 50 Ω impedance at the coaxial output port. The tapered coaxial impedance transformer is simulated and optimized using HFSS to achieve minimum reflection at the sum port, and the results are shown in Fig. 6.

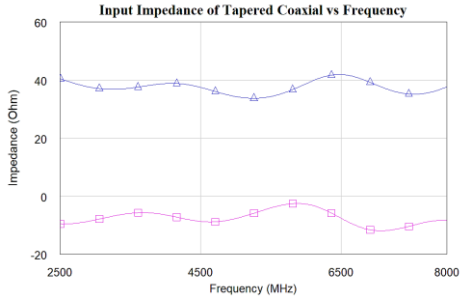

Fig. 6. The input impedance of tapered coaxial impedance transformer vs. frequency, when the output port is terminated with 50 Ω load.

III. The Simulation Results of Power Combiner

For a 16-way power combiner, the slots of the tapered antipodal slotline array are distributed radially around the center of the power combiner, with a radius of 32mm and a degree of 22.5° between each neighboring slot. At the center of the combiner structure, the inner conductor of a conical transmission line is placed. The outer conductor of the conical transmission line and radial waveguide is realized with a bulky metal cap. The overall structure of the designed power combiner is demonstrated in Fig. 7.

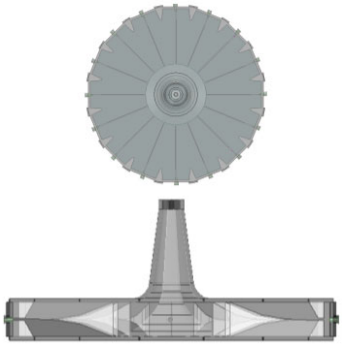

Fig. 7. Top and side view of designed power combiner structure.

Table 1. Font sizes for papers. Table caption with more than one line must be justified. Table caption with just one line must be centered.

The final radial power combiner structure is simulated as a whole in HFSS. The simulated reflection coefficient parameter result for 16-way combiner is shown in Fig. 8.

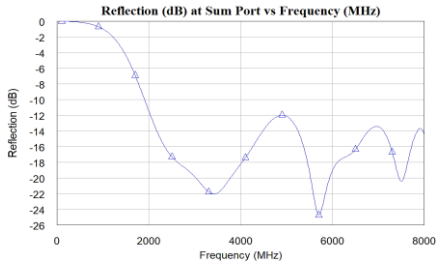

Fig. 8. The simulation results for reflection coefficient parameter (dB) at sum port vs. frequency (MHz).

Simulation results demonstrate that the reflection coefficient at the sum port is lower than -12dB for the wide operating frequency bandwidth. According to simulation results, Sn1 (dB) parameter n=2,3…17 for each way is drawn in Fig. 9.

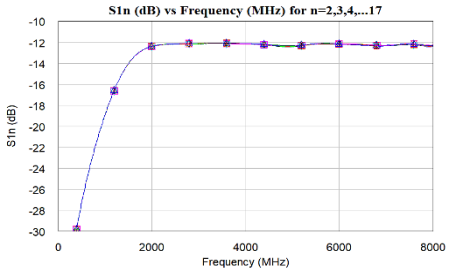

Fig. 9. The simulation results for S1n parameter (dB) vs. frequency (MHz) for n=2,3,4…17.

IV. Measurement Results

S-parameters of the fabricated power combiner were measured using Agilent E5071C network analyzer. The reflection coefficient at the sum port is measured as shown in Fig. 11. The reflection at the sum port of the power combiner is below -11.4 dB.

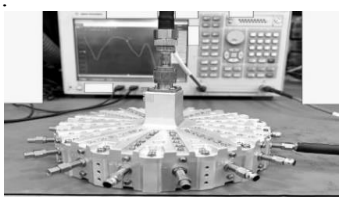

Fig. 10. Fabricated RF power combiner is measured using Agilent E5071C network analyzer.

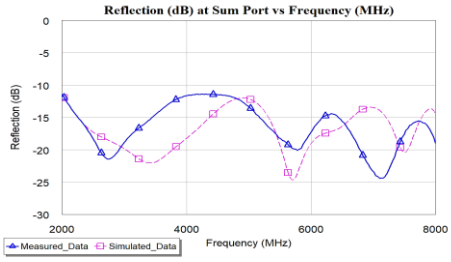

Fig. 11. The simulated and measured reflection coefficient (dB) vs. frequency (MHz), the all input ports are terminated with 50 Ω loads.

By using a 2-port network analyzer, s2p files between the sum port and input port, as well as within the input ports, were obtained. Using these s2p files, s17p file was generated on Cadence Microwave Office (MWO). To calculate the combination loss of the combiner, identical signals at 0 phase angle and -12 dBm amplitude were applied to the input ports at MWO and the difference from the 0 dBm signal power was calculated at the sum port. For an ideal case, there must be a 0 dBm power level at the sum port. The difference between the ideal case and the analysis shows us the combination loss of the fabricated combiner. The results of combination loss for a simulated and measured power combiner are shown in Fig. 12. In the operating frequency of a power combiner, the combination loss was measured at 0.5±0.28 dB. The difference between the simulations and measurements was expected since the N and SMA connectors were not included in the simulations.

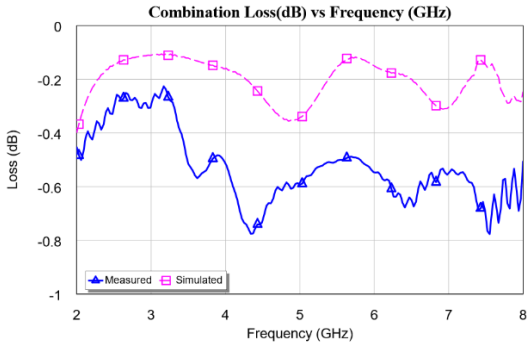

Fig. 12. The simulated and measured combination loss(dB) vs. frequency (GHz), all input ports are fed by the signal that have the same power level and phase angle.

The unbalance between the input ports is measured as less than 1.2 dB. The curves in Fig. 13 demonstrate that minimum and maximum values of the Sn1(dB) measurements for n=2,3,4…17. All Sn1 measurements are inside the gray area. Even if the power combiner structure is symmetrical, due to fabrication process, an asymmetry in between the input ports is occurred.

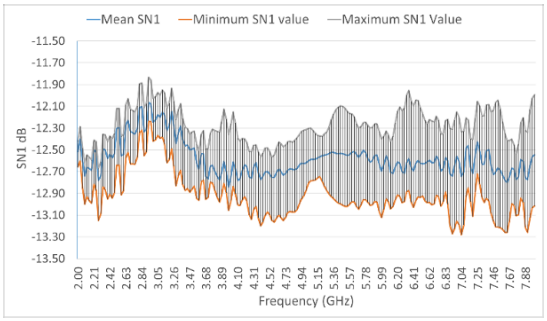

Fig. 13. The minimum and maximum values of Sn1(dB) parameter for n=2,3…17 in each frequency steps at 2-8 GHz operating frequency. All Sn1 measurements are in the gray area.

The isolation parameter between combined ports is measured as less than 8 dB. The structure is symmetric, the isolation of Port 2 from the other input ports are plotted in Fig 14.

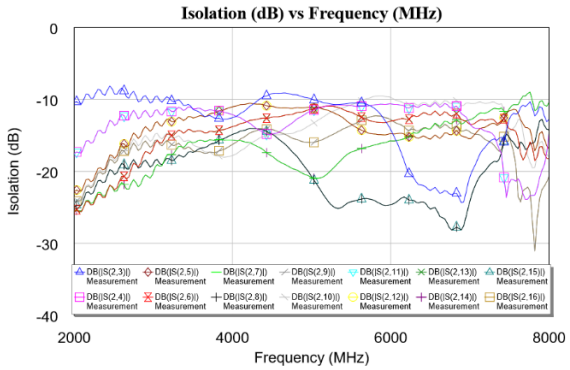

Fig. 14. The measured isolation (dB) between Port 2 and the other input ports vs. frequency (MHz).

This design is a non-isolated RF combiner. If RF power is distributed evenly to all other input ports and the sum port after being injected at one input port, the optimal isolation parameter condition can be attained. In such case, 12dB can be computed as the ideal degree of isolation for a 16-way combiner. In that structure, the injected RF power at one input port is not distributed equally to the other input ports, therefore the isolation value for various input port pairs are not the same and in the worst case, 8 dB is measured.

V. Conclusion

A wideband 16-way spatial power combiner using tapered slotline array in a radial waveguide is designed and is optimized in HFSS EM Simulator. The proposed combiner is fabricated and the results are measured. A good agreement between the simulation and the measurement results is obtained. The proposed model has an advantage of displacing power amplifiers on a large cooling plane.

References

[1] M. Cicolani and A. Panariello, "Novel Design Technique for Radial Power Combiners." *2000 30th European Microwave Conference*, 2000, pp. 1-4.

[2] A. E. Fathy, Sung-Woo Lee and D. Kalokitis, "A simplified design approach for radial power combiners," in *IEEE Transactions on Microwave Theory and Techniques,* vol. 54, no. 1, pp. 247-255, Jan. 2006.

[3] Pengcheng Jia, Lee-Yin Chen, A. Alexanian and R. A. York, "Broad-band high-power amplifier using spatial power-combining technique," in *IEEE Transactions on Microwave Theory and Techniques,* vol. 51, no. 12, pp. 2469-2475, Dec. 2003.

[4] A. Alexanian and R. A. York, "Broadband waveguide-based spatial combiners," *1997 IEEE MTT-S International Microwave Symposium Digest,* 1997, pp.1139-1142, vol. 3.

[5] S.E. Hosseini and Ali Banai, "Ultrabroadband power amplifier using 16-way spatial combining finline array," *Microwave and Optical Letters, vol.* 55, 2013.

[6] H. Javadi-Bakhsh and R. Faraji-Dana, "A wideband twenty element microwave spatial power combiner," *Scientia Iranica*, vol. 21, pp. 853-860, 2014.

[7] D. I. L. de Villiers, P. W. van der Walt and P. Meyer, "Design of a Ten-Way Conical Transmission Line Power Combiner," in *IEEE Transactions on Microwave Theory and Techniques,* vol. 55, no. 2, pp. 302-308, Feb. 2007.

[8] R. D. Beyers and D. I. L. de Villiers, "Design and analysis of an impedance tapered conical to coaxial transmission line transition," *2014 44th European Microwave Conference*, 2014, pp. 307-310.